

The effect of magnesium on the alite phase structural stability and its hydration process

E. Gharibi¹, M. Jabri^{1;2}, A. Ramdani¹

1: Laboratory of Solid, Mineral and analytical chemistry, Faculty of Sciences, Mohamed First University, Oujda-Morocco.

2: LafargeHolcim Company (Morocco).

Received 01Jan 2017,
Revised 17 Feb 2017,
Accepted 18 Feb 2017,

Keywords

- ✓ Magnesium,
- ✓ Calcium,
- ✓ Silicates,
- ✓ Alite,
- ✓ C₃S,
- ✓ Portland cement,
- ✓ Hydration.

gharibi_elkhadir@yahoo.fr
jabrimeid@hotmail.fr

Abstract

In our study we have evaluated the effect of magnesium (Mg) insertion on the stability and the hydration process of tri-calcium silicate which is considered as the main phase of Portland cement clinker. We have concluded that the substitution of calcium by magnesium in the silicate phase involves several phenomena, such as a weak increase of portlandite (Ca(OH)₂) rate, a diminution of the Ca/Si ratio and an augmentation of the average silicate chain lengths. In addition, we have concluded that these aspects are due only to the dopage of Mg into C₃S and not to the alteration of its hydration mechanism. Then, we confirmed that the insertion of Mg is beneficial to maintain the stability of C₃S. At first, we synthesized a pure and doped product with Mg and then studied the effect of Mg insertion on the stability and the hydration of C₃S. Many investigation techniques have been used such as: X-ray diffraction XRD, thermogravimetric analysis TGA, differential Scanning Calorimetry DSC, nuclear magnetic resonance ²⁹Si MAS-NMR and Electron Probe Micro-Analyzer (EPMA).

1. Introduction

The clinker of Portland cement is mainly consisted of several oxides such as CaO, SiO₂, Al₂O₃, Fe₂O₃, MgO, K₂O, Na₂O, SO₃,... which have a shorthand form as C, S, A, F, M, K, N, S respectively. The four main oxides are combined with each other in mineral phases: Alite/C₃S, belite/C₂S, aluminates/C₃A and aluminoferrite/C₄AF. All phases represent about 95% of clinker total mass, however the remaining 5% is consisted of minor elements as M, S, K, N and others, which inevitably modified clinker properties. We are more interested in MgO as the most frequently existing minor component in industrial clinkers and having a great influence on its properties [1, 2]. Indeed, introduced in raw meal with an optimum rate of about 2-3 wt.%, it improves its burnability [3], lowers the melting temperature, increases the quantity of the liquid phase during the clinker's sintering process [1,4 ,5] and promotes the absorption of free lime and the formation of C₃S [3]. Nevertheless when the content of MgO is more than 3 wt.%, it can reduce the burnability of raw meal, increase the content of free lime in clinker and decrease the strength of cement. In addition, a higher content of MgO can impair the soundness of cement [6, 7, 8]. Indeed, during the pyroprocessing of the raw materials, while a part of MgO is stabilized as a solid solution in C₃S, C₂S, and clinker liquid phase, an excess MgO crystallizes out as magnesia (i.e., periclase) during the cooling of clinker [9,34] and can affect the quality of cement by expansion.

Many studies have shown that, at high temperature, Mg is more abundant in the alite [10, 11, 12, 13] and can substitute calcium [11]. In Ca₃SiO₅, the substitution limit of calcium by magnesium is determined by HAHN *et al.* and could be about 1.5 wt.% at 1420°C, 2 wt.% at 1500°C [11], and at 1550 °C the limit is 2.5 wt.% [12, 13]. In 1952, JEFFERY *et al.* had established that the alite had as a chemical formula C₅₄S₁₆AM [3]. This stipulates the existence of a wide solid solution of tricalcium silicate, MgO and aluminium.

The structure and chemistry of M-S-H is significantly different from the structure of C-S-H [14,33] and recently a lot of investigations are focused on the MgO- C₃S system that align the growing interest for using magnesium silicate hydrate (M-S-H) as potential low-pH cements [15] for e.g. nuclear-waste encapsulation [16, 32]. Indeed, Cements with lower pH values help to improve the compatibility with its environment and zone contact, the case of the clay barrier which the cements can prevent the formation of an extended alkaline plume [17].

One other promising approach is to develop alternative low-carbon cementing materials [18, 19, 20]. This includes a group of recently developed reactive MgO cement, which has been reported to have the potential of absorbing CO₂, with a high capacity of combining a large volume of industrial wastes, and recyclability [21,22].

Nowadays, our understanding about the system MgO- C₃S should be extended in order to more greatly expand the uses of portland cement, so our contribution is to carry out the synthesis of doped products with magnesium and then study the insertion effect on the structural stability and the hydration process of calcium silicate phase.

2. Materials and methods

2.1. The synthesis of a pure silicate

At first, we synthesized a pure tri-calcium silicate phase by a stoichiometric mixture of 3CaO-SiO₂ in which the rate of calcium oxide CaO and amorph silicate SiO₂ are 73.7 wt.% and 26.3 wt.% respectively. Calcium oxide is obtained by heating CaCO₃ at 800°C. The mixture is introduced in a melting-pot consisted of platinum at 1450°C for 24 hours. The operation is repeated six times in each one the mixture is quenched and ground at ordinary temperature.

2.2. The synthesis of the silicate doped with magnesium

We have then doped Mg inside the C₃S structure by annealing a mixture consisted of 98% of C₃S and 2% of MgO (MgCO₃) at 1450°C for 24 hours. The operation is repeated again three times, in each one the product is quenched and ground. The analysis by Electron Probe Micro-Analyser (EPMA) of the doped product shows that it is monophasic with a rate of 1.2 wt.% of MgO.

The analysis by X-ray diffraction of C₃S and C₃S doped with MgO is shown in (figure 1) and (figure 2) respectively. All x-ray determinations are made by reflexion and we have used as instrument a diffractometer with curve detector Enraf-Nonius equipped with a cobalt anticathode ($\lambda_{Co} = 1,7890 \text{ \AA}$). So by using the x-ray diffraction technic we have checked the purity of synthesized products and then identified their hydrated forms. Spectra are converted and treated with Diffract-At software with JC-PDF database. The analysis by XRD shows that the pure synthesized products and that doped with Mg are Ca₃SiO₅ triclinic fig.A.1 and Ca₃SiO₅ monoclinic figure -2 respectively. The hydration process is carried out on 1, 3, 7, 21 and 28 days with the water/cement ratio equal to 0,7 and is evaluated by thermogravimetry analysis TGA and Differential Scanning Calorimetry DSC. The nuclear magnetic resonance ²⁹Si MAS-MNR has been used to determine the silicon environment in the gel structure formed after the hydration process.

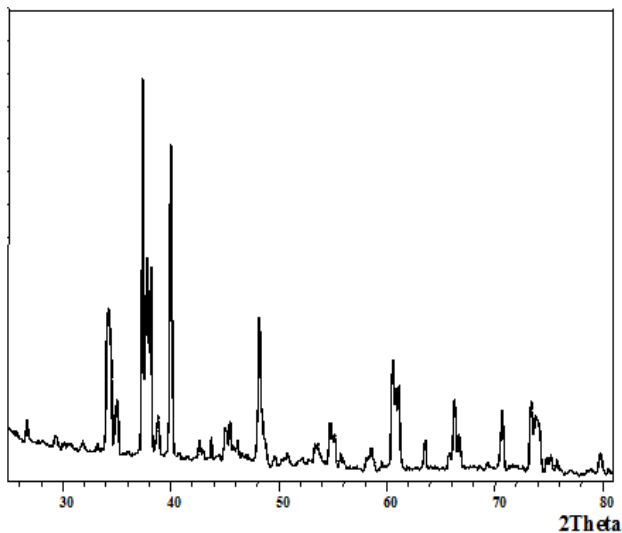


Figure1: Xray diffraction of pure C₃S

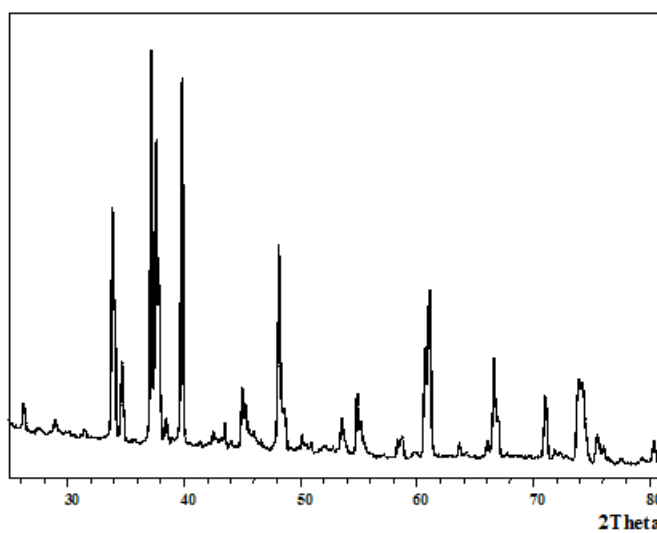


Figure.2: Xray diffraction of C₃S doped with 2 wt.% of MgO

3. Results

3.1. Hydration of tri-calcium silicate

We have studied the hydration of the pure tri-calcium silicate and that doped with 2wt.% of magnesium using the water/cement ratio equals to 0,7. The reaction mechanism of alite hydration can be expressed with two equations as:



In the case of $C_3S_2H_3$ or $C_3S_2H_4$ which are widely responsible of the hydraulic properties of Portland cement, they are considered as the main compounds that determine the setting time of cement. Found as a gel, they have as a general chemical formula $C_xS_yH_z$, in which x, y and z are changeable variables during the hydration process.

3.2. Study by Differential Scanning Calorimetry DSC

In figure 3, they are presented the Differential Scanning Calorimetry DSC analysis of the hydrated pure C_3S and that doped with Mg on 3 days and 21 days.

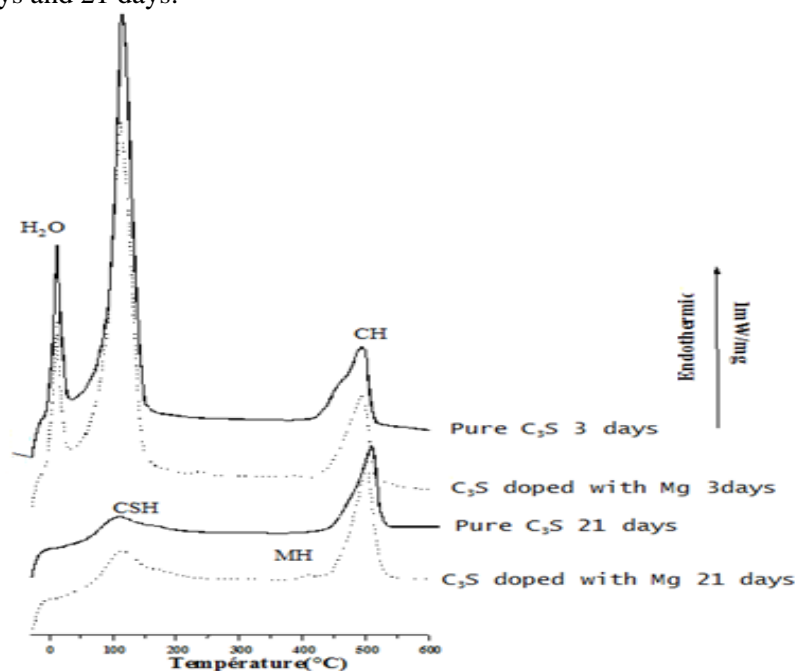


Figure3:DSC curves of hydrated forms of pure C_3S and doped with Mg on 3 and 21 days (water/cement ratio equals to 0,7)

For three days of the hydration process, the Differential Scanning Calorimetry curves related to the pure product and that doped with Mg show three peaks: The first peak between -2 and 10°C is attributed to the fusion of ice[28], the second one which is appeared between 40 and 150°C is due to the evaporation of not bonded water molecules [29] and to the dehydration of CSH gel [30]. The third peak from 420 to 550°C is attributed to the dehydration of portlandite $\text{Ca}(\text{OH})_2$ [31]. Whereas two smallest additional peaks appeared only on the doped samples with Mg: The first peak which sets between 200 and 300°C reveals the decomposition of chemical species in solution before their combination. However, the second which appeared between 350 and 420°C reveals the decomposition of $\text{Mg}(\text{OH})_2$.

For the hydrated products after 21 days, the curves don't show any existence of free water, but instead of a thin peak between 40 and 150°C , they figure out a large hump which shows that the hydration process is carried out on a wide range of temperature and that the compound which decomposes in this zone of temperature presents a wide variety in its composition, as in the case of the CSH gel. For the doped C_3S , the peak associated to the decomposition of $\text{Mg}(\text{OH})_2$ increases and becomes bigger over the time from 3 days to 21 days of hydration process.

3.3. Study by thermogravimetric analysis TGA

In figures 4 and 5 are shown the thermograms of the hydrated forms of the pure C_3S and that doped with magnesium after 21 days respectively. The curves show three loses of weight: The first about 100°C and is due to the dehydration of CSH gel by the evaporation of free water. The second loss at 450°C is due to the decomposition of portlandite, and finally the third loss which starts at 600°C is probably due to de carboxylation of calcite CaCO_3 .

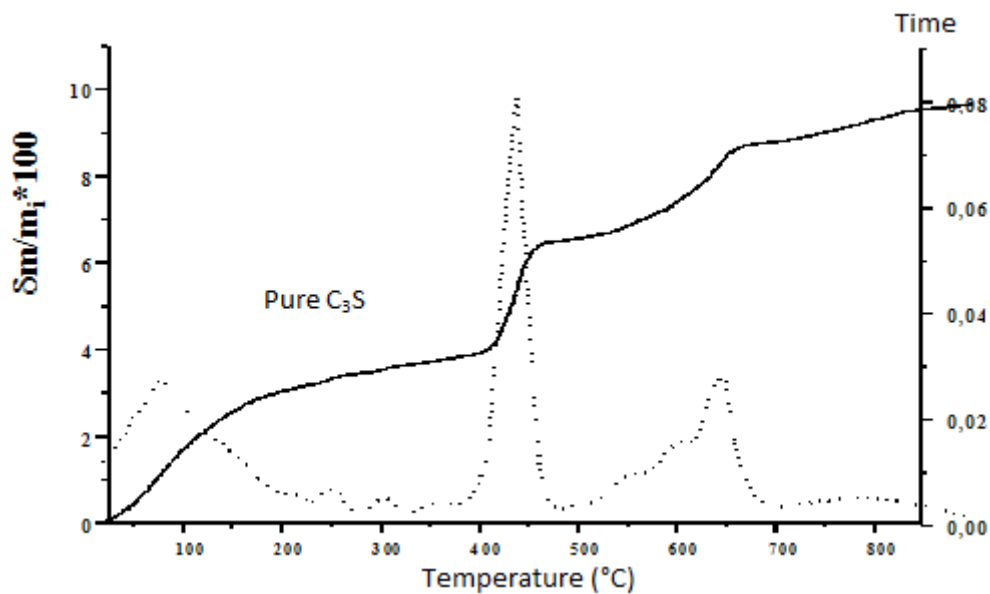


Figure 4: Thermogram of pure C_3S for 21 days (water/cement ratio=0.7)

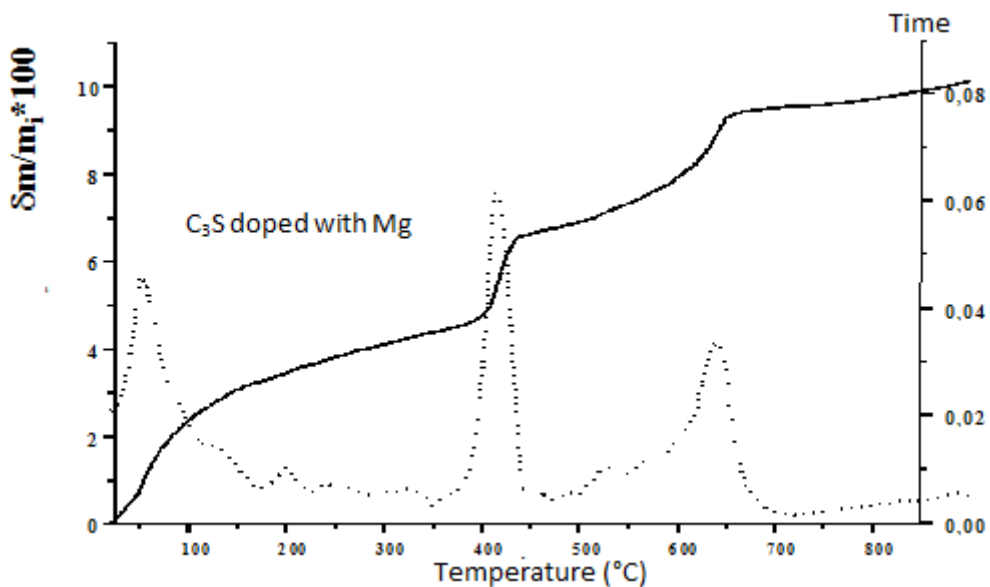


Figure 5: Thermogram of C_3S doped with Mg for 21 days (water/cement ratio=0.7)

3.4. Study by nuclear magnetic resonance ^{29}Si MAS-MNR

In (figure 6) are presented the ^{29}Si -MNR spectra of the pure C_3S and that doped with Mg for 28 days of hydration. They show that both of products have three peaks Q_0 , Q_1 and Q_2 . The Q_0 reveals the existence of monomer tetrahedron SiO_4^{4-} and involves that the tri-calcium silicate is in an orthosilicate form. The second peak Q_1 shows the existence of dimers and tetrahedrons at the limit of the chain. Finally Q_2 reveals the existence of pentamers or likely tetrahedron bonded to two other tetrahedrons. In addition, the ^{29}Si MAS-MNR has served to demonstrate that the C-S-H formed after the hydration of C_3S doped with Mg has quite content of calcium compared to the pure C_3S .

In (figure 7), there is a difference on the form of Q_0 between the pure C_3S and that doped with Mg. This later has a continued and broad peak without disintegration. However the pure one has a Q_0 under multiple peaks (divided into five signals).

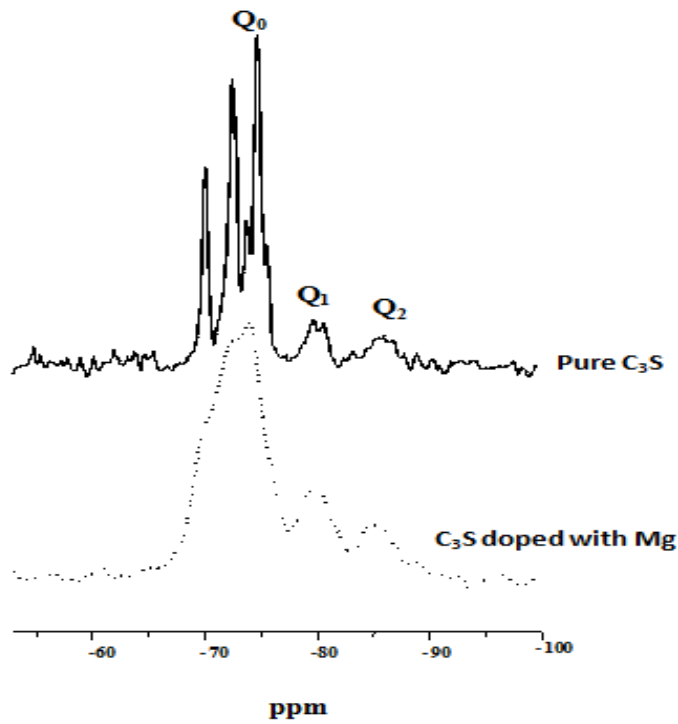


Fig.6: ^{29}Si MAS-MNR spectra of the pure C_3S and that doped with Mg for 28 days (Water/cement ratio = 0,7)

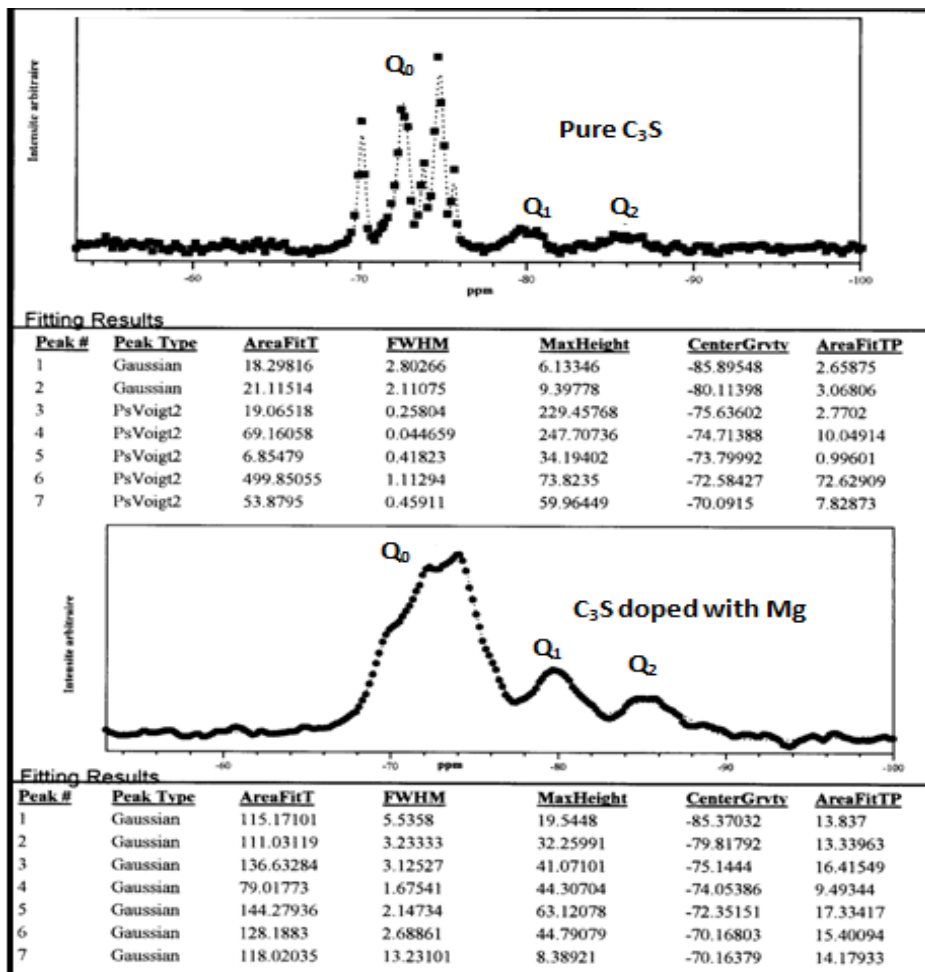


Figure7: Analysis of the ^{29}Si MAS-MNR spectrum peaks of pure C_3S and that doped with Mg for 28 days (Water/cement ratio = 0.7)

4. Discussion

In tri-calcium silicate the magnesium can substitute calcium and promote a considerable stability of the structure. Likely the C_3S changes from triclinic to monoclinic when is doped with Mg. The XRD characteristic peaks of C_3S triclinic phase (T1) are:

- $36.5^\circ \leq 2\theta \leq 38.25^\circ$ 303, 04-4, 042, 40-2
- $60.0^\circ \leq 2\theta \leq 62.00^\circ$ 0-82, -4-46, 4-4-4

These peaks are indexed after transformation into monoclinic lattice (M3) with:

- $36.5^\circ \leq 2\theta \leq 38.25^\circ$ -606, -12.00, -224
- $60.0^\circ \leq 2\theta \leq 60.00^\circ$ 14.24, 040 [1, 24]

In (figure 8) are presented the XRD spectra of the pure C_3S and that doped with Mg in the specified zones mentioned above. Recording to TAYLOR [1], all the varieties of C_3S have identical structures, more specifically in the positions of Ca^{2+} , O^{2-} and Si^{4+} . The difference is only in the orientation of SiO_4^{4-} tetrahedrons which exist at any disordered structure.

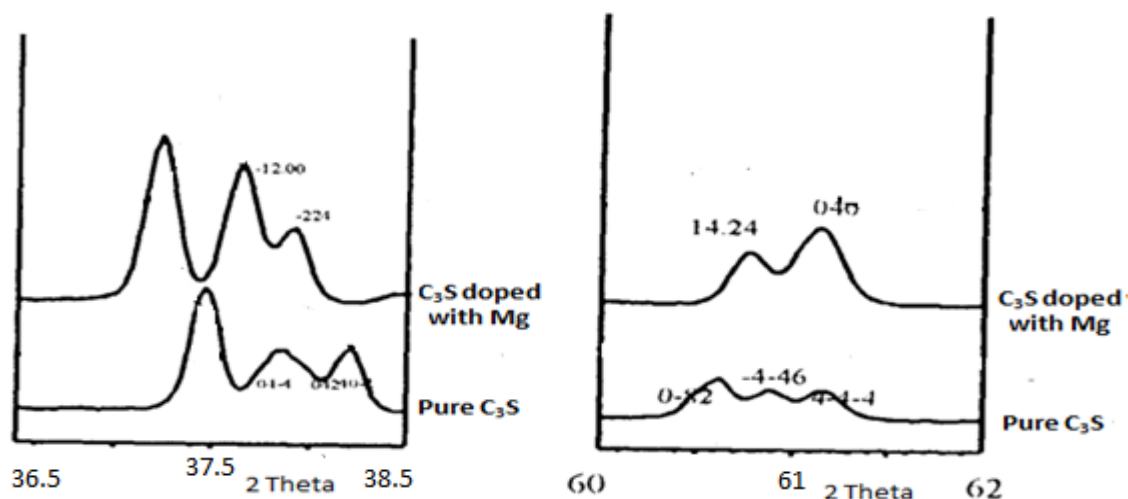
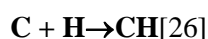
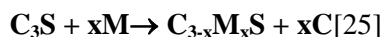
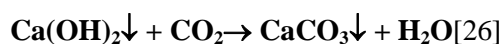


Figure8: X ray diffraction of the pure C_3S and that doped with Mg in the specific regions of 2-theta

The hydration kinetic of the pure C_3S and that doped with Mg shows a little difference, however, the rate of portlandite $Ca(OH)_2$ formed after hydration process in the case of C_3S doped with Mg is pretty higher than the pure one. These results are presented in the (figure 9) which shows the formation of portlandite after 3 and 21 days of hydration process of the pure C_3S and that doped with Mg. Indeed, the insertion of magnesium into alite could be the origin of this difference. While Mg substitutes Ca, a part of calcium reacts with water to form the portlandite $Ca(OH)_2$ following the two reactions below:



In opposite we have observed that the quantity of portlandite decreases between 3 and 21 days. This is could be explained by the carbonation of portlandite with CO_2 from air. Indeed, after hydration, the paste of cement contacts the CO_2 of the air which triggers the transformation of $Ca(OH)_2$ into the calcite as the following reaction:



The presence of carbonate is revealed over $600^\circ C$ by TGA for both samples: the pure C_3S and that doped with Mg.

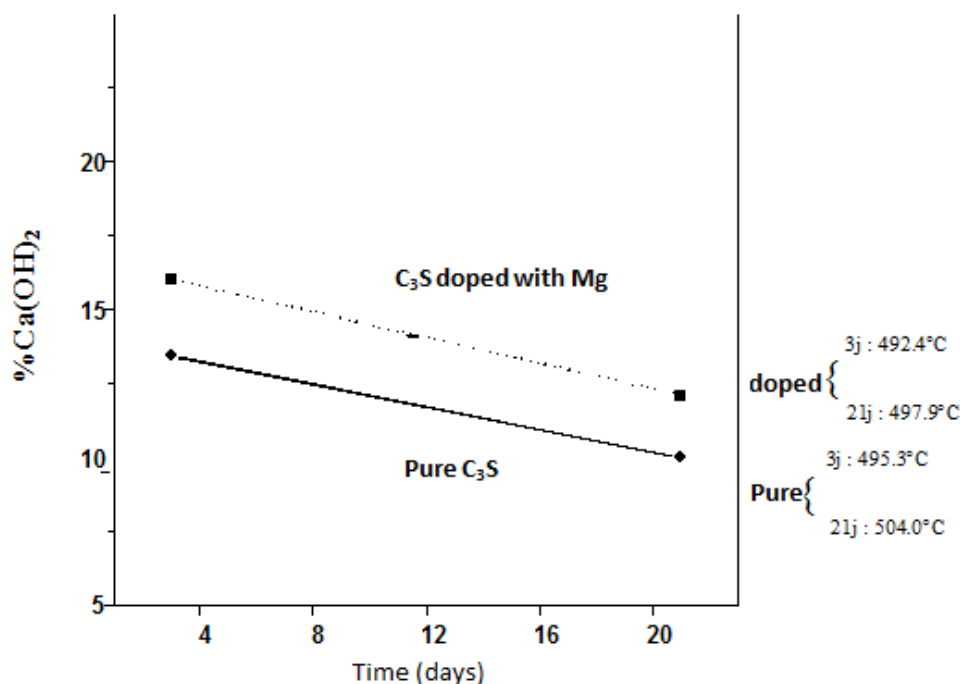


Figure9: The rate of portlandite formed in case of the pure C_3S and that doped with Mg after 3 and 21 days of hydration (water/cement ratio = 0,7)

The nuclear magnetic resonance provides interesting information such as the area of peaks Q_1 and Q_2 , related to the monomers and dimmers respectively. On this light we have determined the length average of silicate chains and the Ca/Si ratio of the gels. The table 1 sums up the analysis of peak airs relative to the pure C_3S and that doped with Mg.

Table 1: The airs of Q_1 and Q_2 of pure C_3S and that doped with Mg determined from TGA curves.

Pure C_3S		C_3S doped with Mg	
Q_1	21.115	Q_1	111.031
Q_2	18.298	Q_2	115.17

The average silicate chain lengths ASCL equation (B.1) and the Ca/Si ratio equation (B.2) of tobermorite of the same gel are determined by using the empiric formula established by RICHARDSON *et al.* [27]. We have obtained the following values as summed up in table 2:

$$ASCL = 3n-1 = 2(Q_1+Q_2)/Q_1 \quad (B.1)$$

$$Ca(T_{(3n-1)})/Si = 5n/2(3n-1) = 5(2 + Q_1/Q_1+Q_2)/12 \quad (B.2)$$

Table 2 : ASCL and Ca/Si ratio of pure C_3S and that doped with Mg

Pure CSH		CSH doped with Mg	
ASCL	Ca/Si	ASCL	Ca/Si
3.73	1.06	4.03	1.04

For the calcul of Ca/Si ratio, we have obtained a small difference between pure alite and that doped with Mg in favor of the first which is superior than the doped one. In addition, the value of $\Delta(Ca/Si)$ equation (B.3) which equals to 1,89 wt.% is coherent with 1.77 wt.% Mg obtained by using the microsonde analysis. As a

consequence the quantity of gel formed is poor on calcium substituted by magnesium introduced in the Ca_3SiO_5 structure. That what obviously we have found:

$$\Delta(\text{Ca/Si}) = [\text{Ca/Si (pure)} - \text{Ca/Si (doped)}] / (\text{Ca/Si (pure)}) = 1.89 \% (\text{B.3})$$

Conclusion

In this work we have studied the effect of the insertion of Mg into pure alite structure and its effect on the stability and hydration process. We have checked that Mg is beneficial to keep the stability of C_3S phase by transformation from triclinic to monoclinic form. On the other side, we have concluded the weak increase of portlandite rate, the augmentation of the average silicate chain lengths and the diminution of the Ca/Si ratio are due to the doping of Mg into C_3S and not to the alteration of its hydration mechanism.

References

1. Taylor H. F. W., Cement chemistry, *Thomas Telford.*, (1997).
2. Zhang J., Gong Ch., Lu L., Wang S., Hou P., *Ceramics – Silikáty*, 59 (2) (2015) 135-144.
3. Xiaocun Liu, Yanjun Li, *Cem. Concr. Res.*, 35 (2005) 1685-1687.
4. Xuerun Li, Hong Huang, Jie Xu, Suhua Ma, Xiaodong Shen, *Constr. Buil. Mat.*, 37 (2012) 548-555.
5. Altun A.I., *Cem. Concr. Res.* 29 (1999) 1867.
6. Li X., Wenlong Xu, Shaopeng Wang, Mingliang Tang, Xiaodong Shen, *Constr. Buil. Mat.*, 58 (2014) 182–192
7. De la Torre A.G., De Vera R.N., Cuberos A.J.M., Aranda M.A.G., *Cem. Concr. Res.*, 38 (2008) 1261.
8. Xiaocun Liu, Yanjun Li, *Cem. Concr. Res.*, 35 (2005) 1685–1687.
9. Katyal N.K., Ahluwalia S.C., Parkash R., Sharma R.N., *Cem. Concr. Res.*, 28 (4) (1998) 481-485.
10. Stephan D., Wistuba S., *Journ. of the European Ceramic Society*, 26 (2006) 141-148.
11. Hahn T., Eysel W., Woermann E., *5th ISCC.*, 1 (1969) 61-67.
12. Woermann E., Hahn T., Eysel W., *Zement- Kalk-Gips.*, 16 (1963) 370-375.
13. Guinier A., Regourd M., *5th ISCC.*, 1 (1969) 1-43.
14. Lothenbach B., Nied D., L'Hôpital E., Achiedo G., Dauzères, *Cem. Concr. Res.*, 77 (2015) 60-68.
15. Dominik Nied, Kasper Enemark-Rasmussen, Emilie L'Hopital, Jørgen Skibsted, Barbara Lothenbach. *Cem. Concr. Res.* 79 (2016) 323-332.
16. Zhang, Vandepierre L.J., Cheeseman C.R., *NUWCEM.*, (2011) 582-591.
17. Berner U., Kulik D.A., Kosakowski G., *Phys. Chem. Earth* 64 (2013) 46-56.
18. Scrivener K.L., Kirkpatrick R.J., *Cem. Concr. Res.*, 38 (2008) 128-136.
19. Juenger M.C.G., Winnefeld F., Provis J.L., Ideker H.H., *Cem. Concr. Res.*, 41 (2011) 1232-1243.
20. Liwu Moa, Feng Zhang, Min Deng. *Construction and Building Materials* 96 (2015) 147-154.
21. Harrison J. W., *PCT, AU.*, 00077 (2001).
22. Liska M., Al-Tabbaa A., *Proc. Inst. Civil Eng. Waste Resour. Manage.*, 162 (2009) 185-196.
23. Jeffery J.W., *3th ISCC.* (1952) 31-49.
24. Maki I., Kato K., *Cem. Concr. Res.*, 12 (1982) 93-100.
25. Brunauer S., Greenberg A., *4th ISCC.*, 1 (1960) 135-165.
26. Chen D., Dollimore D., *J. Thermal. Anal.*, 44 (1995) 1001-1011.
27. Richardson I.G., Groves G.W., *Cem. Concr. Res.*, 22 (1992) 1001-1010.
28. Boikova A.I., *8th ISCC.*, 1 (1986) 19-35.
29. Glasser F.P., Marr J., *Cem. Concr. Res.*, 10 (1980) 735-758.
30. Boikova A.I., Essayam A., Lazukin V., *7th ISCC.*, 7 (1983) 183-185.
31. Sarkar S.L., Roy D.M., *6th Inter. Conf. Cem. Micros.*, (1984) 37-47.
32. Ludwig H.M., Zhang, W., *Cem. Concr. Res.*, 78 (2015) 24-37.
33. Stephan D., Dikoundou S., Raudaschl-Sieber G., *Thermochimica Acta*, 472 (2008) 64-73.
34. Ren X.; Zhang W.; Ouyang S., *Journal of the Chinese Ceramic Society*. 40 (2012) 664-670.

(2017) ; <http://www.jmaterenvironsci.com>